HOKKAIDO UNIVERSITY

Title	Production cross sections of ytterbium and thulium radioisotopes in alpha-induced nuclear reactions on natural erbium
Author(s)	Saito, Moemi; Aikawa, Masayuki; Sakaguchi, Michiya; Ukon, Naoyuki; Komori, Yukiko; Haba, Hiromitsu
Citation	Applied Radiation and Isotopes, 154, 108874 https://doi.org/10.1016/j.apradiso.2019.108874
Issue Date	2019-12
Doc URL	http://hdl.handle.net/2115/82507
Rights	©2019. This manuscript version is made available under the CC-BY-NC-ND 4.0 license http://creativecommons.org/licenses/by-nc-nd/4.0/
Rights(URL)	https://creativecommons.org/licenses/by-nc-nd/4.0/
Type	article (author version)
File Information	ARI154_108874.pdf

Instructions for use

Hokkaido University Collection of Scholarly and Academic Papers : HUSCAP

Production cross sections of ytterbium and thulium radioisotopes in alpha-induced nuclear reactions on natural erbium

Moemi Saito[a,*], Masayuki Aikawa[a,b], Michiya Sakaguchi[c,1], Naoyuki Ukon[d], Yukiko Komori[e], Hiromitsu Haba[e]

[a] *Graduate School of Biomedical Science and Engineering, Hokkaido University, Sapporo 060-8638, Japan*

[b] *Faculty of Science, Hokkaido University, Sapporo 060-0810, Japan*

[c] *School of Science, Hokkaido University, Sapporo 060-0810, Japan*

[d] *Advanced Clinical Research Center, Fukushima Medical University, Fukushima 960-1295, Japan*

[e] *Nishina Center for Accelerator-Based Science, RIKEN, Wako 351-0198, Japan*

Abstract

Activation cross sections of alpha-induced reactions on natural erbium were measured using a 50.9-MeV alpha-beam at the RIKEN AVF cyclotron. Well-established methods for the measurements, the stacked-foil activation technique and gamma-ray spectrometry, were used. Production cross sections of ^{166,169}Yb and ^{165,166,167,168,170,173}Tm were determined. This is the first measurement of the cross sections of ^{166,170}Tm. The integral yield of the medical radionuclide ^{169}Yb was derived from the measured excitation function.

Keyword

Ytterbium-169; Alpha irradiation; Erbium target; Excitation function; Cross section

1. Introduction

Radionuclides can be used in application fields such as engineering and medicine. The production reactions of such radionuclides should be investigated for practical use. The best way of the production can be discussed based on excitation functions of a variety of possible nuclear reactions.

The radionuclide ^{169}Yb ($T_{1/2}$ = 32.018 d) is one of the medical radionuclides. It decays with emission of Auger electrons and X-rays, which can be used for brachytherapy (Leonard et al., 2011). There are several reactions to produce ^{169}Yb. One is the neutron capture reaction on ^{168}Yb in reactors, however it has a disadvantage of low abundance of ^{168}Yb (0.123%) in natural ytterbium. Charged-particle induced reactions on erbium and thulium targets allow for production of ^{169}Yb, too. In this

* Corresponding author: Moemi Saito, moemi@nds.sci.hokudai.ac.jp

[1] Present address: Graduate School of Biomedical Science and Engineering, Hokkaido University, Sapporo 060-8638, Japan

paper, we focused on the alpha-induced reactions on ^{nat}Er (^{162}Er: 0.139%, ^{164}Er: 1.601%, ^{166}Er: 33.503%, ^{167}Er: 22.869%, ^{168}Er: 26.978%, ^{170}Er: 14.910%). Four previous studies of the ^{nat}Er(α,x)^{169}Yb reaction (Archenti et al., 1985; Homma et al., 1980; Király et al., 2008; Sonzogni et al., 1992) could be found in the EXFOR library (Otuka et al., 2014). However, the experimental data published earlier are rather inconsistent. Therefore, we re-measured the excitation functions of the alpha-particle induced nuclear reaction on ^{nat}Er with particular focus on ^{169}Yb. The production cross sections of co-produced radionuclides, ^{166}Yb, and ^{165,166,167,168,170,173}Tm, were also determined. Based on the measured cross sections, the integral yield of ^{169}Yb was calculated from the measured cross-sections.

2. Experimental

The activation cross sections of the alpha-induced reactions on ^{nat}Er were measured. The experiment was performed at the AVF cyclotron of the RIKEN RI Beam Factory. The stacked foil activation method and the gamma-ray spectrometry were used.

The target for the experiment consisted of ^{nat}Er (99% purity, Goodfellow Co., Ltd., UK) and ^{nat}Ti (99.6% purity, Nilaco Corp., Japan). The ^{nat}Ti foils were used for the ^{nat}Ti(α,x)^{51}Cr monitor reactions to assess beam parameters and target thicknesses. The sizes and weights of both foils were measured to estimate their thicknesses. The derived thicknesses of ^{nat}Er and ^{nat}Ti were 20.06 mg/cm^2 and 2.26 mg/cm^2, respectively. The measured foils were cut into 10×10 mm^2 to fit a target holder. The target holder served also as a Faraday cup.

The stacked target was irradiated for 1 hour by a 50.9-MeV alpha-beam at the AVF cyclotron of the RIKEN RI Beam Factory. The energy was measured by the time-of-flight method (Watanabe et al., 2014). The energy degradation in the stacked target was calculated using the SRIM code (Ziegler et al., 2008). The beam intensity measured by the Faraday cup was 200.3 nA. These beam parameters were assessed by the ^{nat}Ti(α,x)^{51}Cr monitor reactions.

Gamma rays emitted from the irradiated foils were measured using two HPGe detectors (ORTEC GEM30P4-70 and ORTEC GMX30P4-70). The detectors were calibrated by a multiple gamma ray emitting point source (Eckert & Ziegler Isotope Products Inc.) consisting of ^{57,60}Co, ^{88}Y, ^{109}Cd, ^{113}Sn ^{137}Cs, ^{139}Ce and ^{241}Am, which cover the energy range between 60 keV and 1836 keV. The gamma ray spectra were analyzed by the dedicated software, Gamma Studio (SEIKO EG&G). Reaction and decay data of the reaction products were taken from NuDat 2.7 (National Nuclear Data Center, 2017), Lund/LBNL Nuclear Data Search (Chu et al., 1999), LiveChart (International Atomic Energy Agency, 2009) and QCalc (Pritychenko and Sonzogni, 2003). The data are summarized in Table 1.

Table 1. Reactions and decay data of reaction products

Nuclide	Half-life	Decay mode (%)	E_γ (keV)	I_γ (%)	Contributing reactions	Q-value (MeV)
^{169g}Yb	32.02 d	ε (100)	63.12044(3)	43.62(23)	^{166}Er(α,n)^{169}Yb	-10.2
			177.21307(4)	**22.28(11)**	^{167}Er(α,2n)^{169}Yb	-16.6
			197.95675(4)	35.93	^{168}Er(α,3n)^{169}Yb	-24.4
					^{170}Er(α,5n)^{169}Yb	-37.7
^{166}Yb	56.7 h	ε (100)	**82.29(2)**	**15.552**	^{162}Er(α,γ)^{166}Yb	-2.3
					^{164}Er(α,2n)^{166}Yb	-18.1
					^{166}Er(α,4n)^{166}Yb	-33.2
					^{167}Er(α,5n)^{166}Yb	-39.6
					^{168}Er(α,6n)^{166}Yb	-47.4
^{173}Tm	8.24 h	β^-(100)	**398.9(6)**	**87.9(9)**	^{170}Er(α,p)^{173}Tm	-8.7

^{170}Tm	128.6 d	β^-(99.87)	**84.25474(8)**	**2.48(6)**	^{167}Er(α,d)^{170}Tm	-8.4
		ε (0.13)			^{168}Er(α,d)^{170}Tm	-13.9
					^{170}Er(α,tn)^{170}Tm	-20.9
^{168}Tm	93.1 d	β^-(0.01)	184.295(2)	18.15(16)	^{166}Er(α,d)^{168}Tm	-14.3
		ε (99.99)	198.251(2)	54.49(16)	^{167}Er(α,t)^{168}Tm	-14.5
			447.515(3)	23.98(11)	^{168}Er(α,tn)^{168}Tm	-22.3
			815.989(5)	**50.95(16)**	^{170}Er(α,t3n)^{168}Tm	-35.5
^{167}Tm	9.25 d	ε (100)	**207.801(5)**	**42(8)**	^{164}Er(α,p)^{167}Tm	-8.3
					^{166}Er(α,dn)^{167}Tm	-21.2
					^{167}Er(α,tn)^{167}Tm	-21.3
					^{168}Er(α,t2n)^{167}Tm	-29.1
					^{170}Er(α,t4n)^{167}Tm	-42.4
^{166g}Tm	7.70 h	ε (100)	184.405(25)	16.2(10)	^{164}Er(α,d)^{166}Tm	-14.8
			705.333(20)	11.1(7)	^{166}Er(α,tn)^{166}Tm	-23.6
			778.814(15)	**19.1(12)**	^{167}Er(α,t2n)^{166}Tm	-27.6
			785.904(15)	10.0(6)	^{168}Er(α,t3n)^{166}Tm	-37.8
			1273.540(16)	15.0(9)		
			2052.36(3)	17.4(11)		
^{165}Tm	30.06 h	ε (100)	**242.917(7)**	**35.5(17)**	^{162}Er(α,p)^{165}Tm	-8.3
			297.369(6)	12.7(6)	^{164}Er(α,t)^{165}Tm	-15.5
					^{166}Er(α,t2n)^{165}Tm	-30.7
					^{167}Er(α,t3n)^{165}Tm	-37.1
					^{168}Er(α,t4n)^{165}Tm	-44.9
^{51}Cr	27.7025 d	ε (100)	**320.0824**	**9.910(10)**		

Cross sections of the ^{nat}Ti(α,x)^{51}Cr monitor reaction were derived to assess the beam parameters and target thicknesses. The gamma line at 320.08 keV (I_γ = 9.910%) from decay of ^{51}Cr ($T_{1/2}$ = 27.7025 d) was measured for the cross sections. The dead time during the measurements was kept less than 1.1% after a cooling time of 12 days. The derived cross sections were compared with the IAEA recommended values (Hermanne et al., 2018) and shown in Fig. 1. We could obtain good agreement with the recommended values using the corrected thickness of ^{nat}Er decreased by 1% within the uncertainty, the measured one of ^{nat}Ti and intensity.

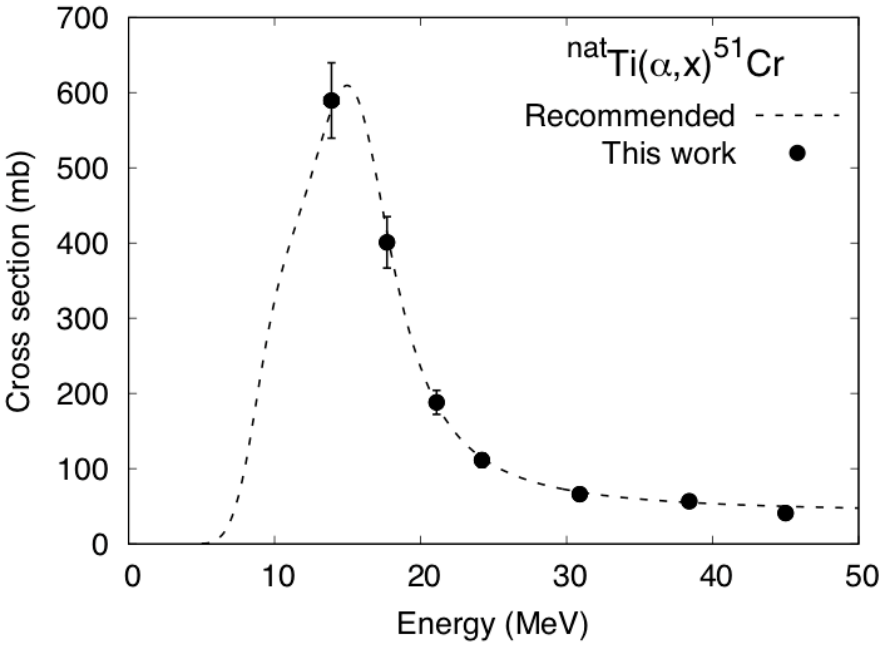

Fig. 1. Excitation function of the $^{nat}Ti(\alpha,x)^{51}Cr$ monitor reaction with the recommended values (Hermanne et al., 2018).

3. Result and discussion

The production cross sections of ^{169}Yb and co-produced radionuclides, ^{166}Yb and ^{165,166,167,168,170,173}Tm, were determined. The numerical data of the measured cross sections are listed in Table 2. The results are displayed in Figs. 2-9 with the previous experimental studies (Archenti et al., 1985; Homma et al., 1980; Király et al., 2008; Sonzogni et al., 1992) and the TENDL-2017 data (Koning et al., 2019). The production yield of ^{169}Yb deduced from the measured cross sections is shown in Fig. 10. The yield was compared with the previously integrated experimental data (Király et al., 2008).

The total uncertainty of the cross sections was estimated to be 8.5-29.0%. It was derived from the square root of the quadratic summation of each component; statistical uncertainty (0.2-27.7%), target thickness (1%), target purity (1%), beam intensity (5%), detector efficiency (6%), γ-intensity (<19%) and peak fitting (3%).

Table 2. Measured production cross sections (mb)

Energy (MeV)	^{169}Yb	^{166}Yb	^{173}Tm	^{170}Tm	^{168}Tm	^{167}Tm	^{166}Tm	^{165}Tm
48.9 ±0.8	170 ±15	414 ±37		14 ±2	31 ±3	531 ±111	95 ±14	23 ±2
47.5 ±0.8	156 ±13	372 ±34		16 ±3	28 ±3	534 ±111	78 ±10	18 ±2
46.1 ±0.8	144 ±12	317 ±29		16 ±3	26 ±2	542 ±113	57 ±8	19 ±2
42.7 ±0.9	186 ±16	153 ±14		11 ±2	22 ±2	572 ±119	23 ±4	24 ±2
41.2 ±0.9	236 ±20	86 ±8	0.39 ±0.04	11 ±2	19 ±2	570 ±119	3.8 ±0.6	22 ±2
39.6 ±0.9	303 ±26	38 ±4	0.42 ±0.04	9.1 ±1.7	18 ±2	559 ±117	2.5 ±0.3	22 ±2
35.8 ±1.0	398 ±34		0.49 ±0.04	7.4 ±1.6	12 ±1	427 ±89		15 ±1
34.1 ±1.0	394 ±34		0.53 ±0.05	8.2 ±1.7	9.3 ±0.9	349 ±73		9.9 ±1.0
32.3 ±1.0	379 ±32		0.56 ±0.05	6.8 ±1.6	6.8 ±0.7	235 ±49		4.5 ±0.4
27.9 ±1.1	263 ±22		0.55 ±0.05	2.8 ±0.8	1.9 ±0.2	8.9 ±1.9		0.26 ±0.04
25.8 ±1.2	218 ±19		0.44 ±0.04	2.3 ±0.6	0.80 ±0.10	2.5 ±0.5		0.35 ±0.04
22.9 ±1.3	172 ±15		0.15 ±0.01		0.11 ±0.04	4.2 ±0.9		0.60 ±0.06
19.7 ±1.4	92 ±8		0.019 ±0.003			3.8 ±0.8		0.35 ±0.04
16.1 ±1.6	6.2 ±0.5					0.31 ±0.07		0.031 ±0.005

3.1 The $^{nat}Er(\alpha,x)^{169}Yb$ reaction

The production cross sections of the $^{nat}Er(\alpha,x)^{169}Yb$ reaction were derived. The radionuclide ^{169}Yb has a metastable state with a short half-life ($T_{1/2}$ = 46 s, IT: 100%), which decays only to the ground state ^{169g}Yb ($T_{1/2}$ = 32.02 d) soon after the end of bombardment. The gamma line at 177.21 keV (I_γ = 22.28%) from the decay of ^{169g}Yb was measured after a cooling time of 11 days. The cross sections were obtained from the net counts of the gamma line and shown in Fig. 2. The results are compared with the previous studies (Archenti et al., 1985; Homma et al., 1980; Király et al., 2008; Sonzogni et al., 1992) and the TENDL-2017 data (Koning et al., 2019). Both data of Király et al. (2008) and TENDL-2017 have nearly the same peak position as ours at around 35 MeV while the amplitudes are different. The other experimental data differ significantly in both the shape and amplitude from our results.

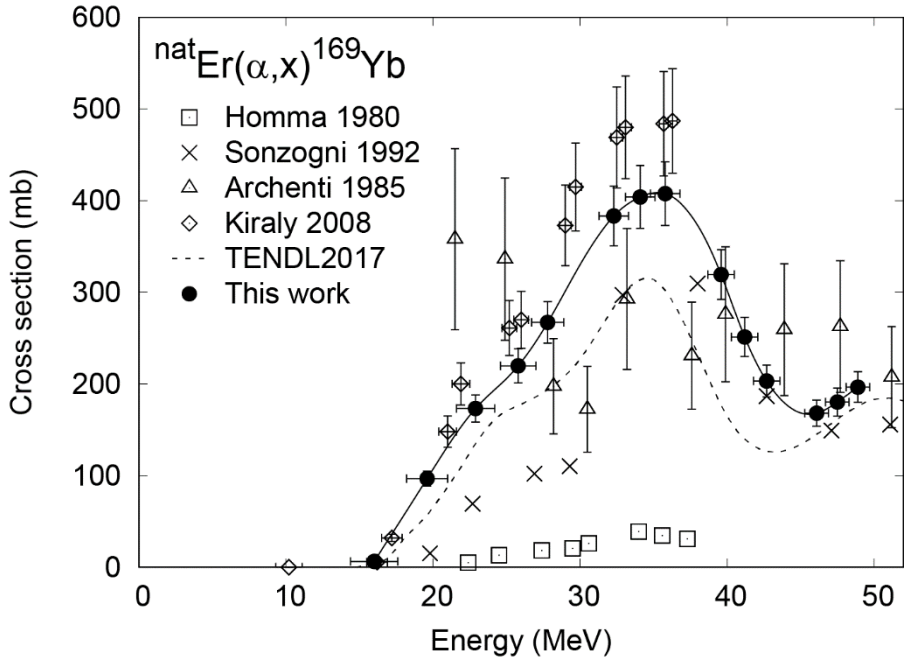

Fig. 2. Excitation function of the $^{nat}Er(\alpha,x)^{169}Yb$ reaction

3.2 The $^{nat}Er(\alpha,x)^{166}Yb$ reaction

The excitation function of the $^{nat}Er(\alpha,x)^{166}Yb$ reaction was derived from the gamma line at 82.29 keV (I_γ = 15.552%) from the decay of ^{166}Yb ($T_{1/2}$ = 56.7 h). The measurements of the gamma line were performed after a cooling time of 11 days to reduce background. The derived excitation function was shown in Fig. 3 with the experimental data studied earlier (Archenti et al., 1985; Sonzogni et al., 1992) and the TENDL-2017 data (Koning et al., 2019). The two previous experimental data are lower than our data. The TENDL-2017 data overestimate all the experimental data including ours.

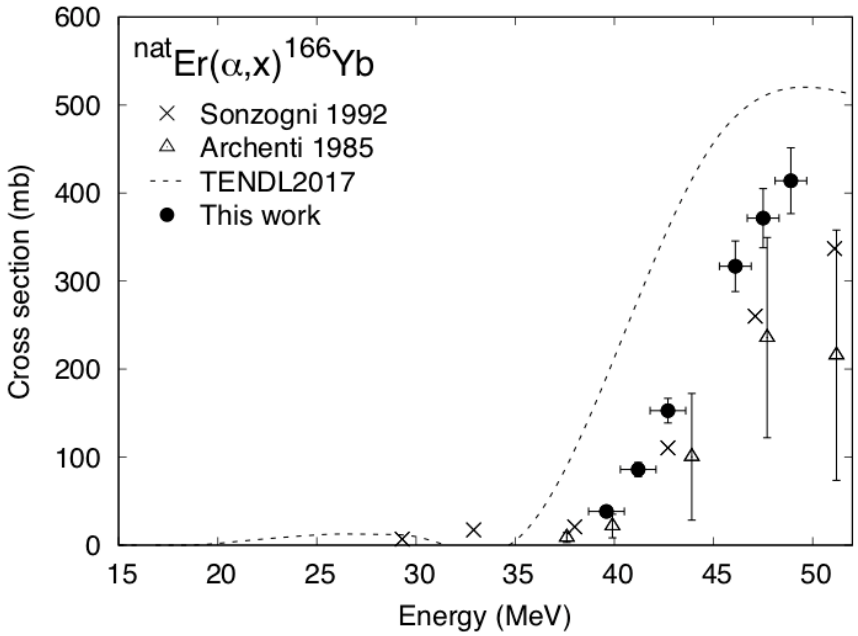

Fig. 3. Excitation function of the $^{nat}Er(\alpha,x)^{166}Yb$ reaction

3.3 The $^{nat}Er(\alpha,x)^{173}Tm$ reaction

The excitation function of the $^{nat}Er(\alpha,x)^{173}Tm$ reaction was derived from measurements of the gamma line at 398.9 keV (I_γ = 87.9%) from the ^{173}Tm decay ($T_{1/2}$ = 8.24 h). The measurements were performed after a cooling time of 2.2 h. The cross sections obtained from the net counts of the gamma line are shown in Fig. 4. The results are compared with the previous study (Király et al., 2008) and the TENDL-2017 data (Koning et al., 2019). The result of the previous study is slightly higher than our result while the peak positions are located at nearly the same energy. The TENDL-2017 data underestimate remarkably the experimental data.

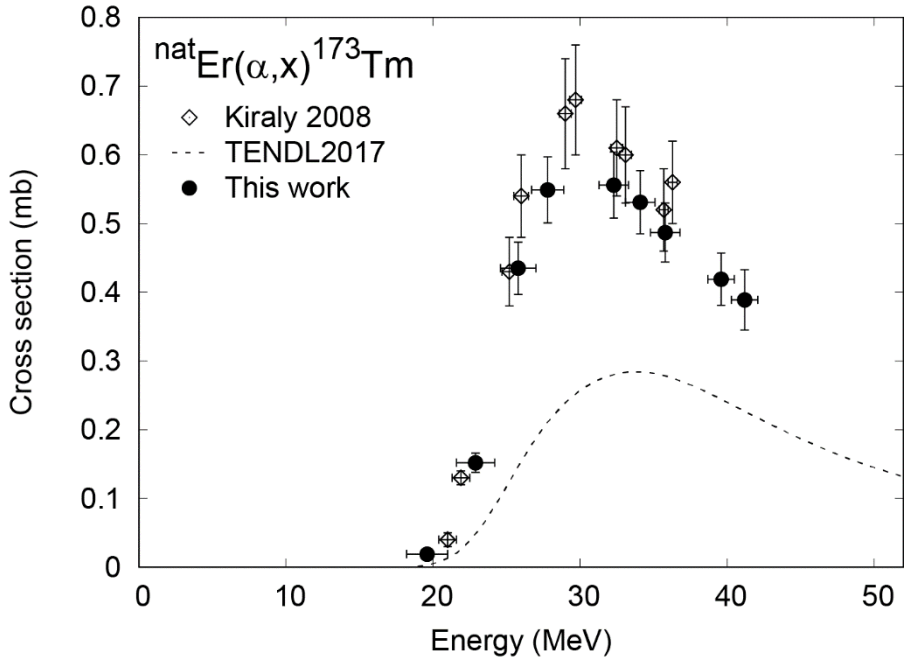

Fig. 4. Excitation function of the $^{nat}Er(\alpha,x)^{173}Tm$ reaction

3.4 The ^{nat}Er(α,x)^{170}Tm reaction

The measurements of the 84.25-keV gamma line (I_γ = 2.48%) from the ^{170}Tm decay ($T_{1/2}$ = 128.6 d) were performed after a cooling time of 247 days. The cross sections of the ^{nat}Er(α,x)^{170}Tm reaction were derived from the measurements. The result is shown in Fig. 5 in comparison with the TENDL-2017 data (Koning et al., 2019). The TENDL-2017 data underestimate our data. There was no experimental study found in the literature survey.

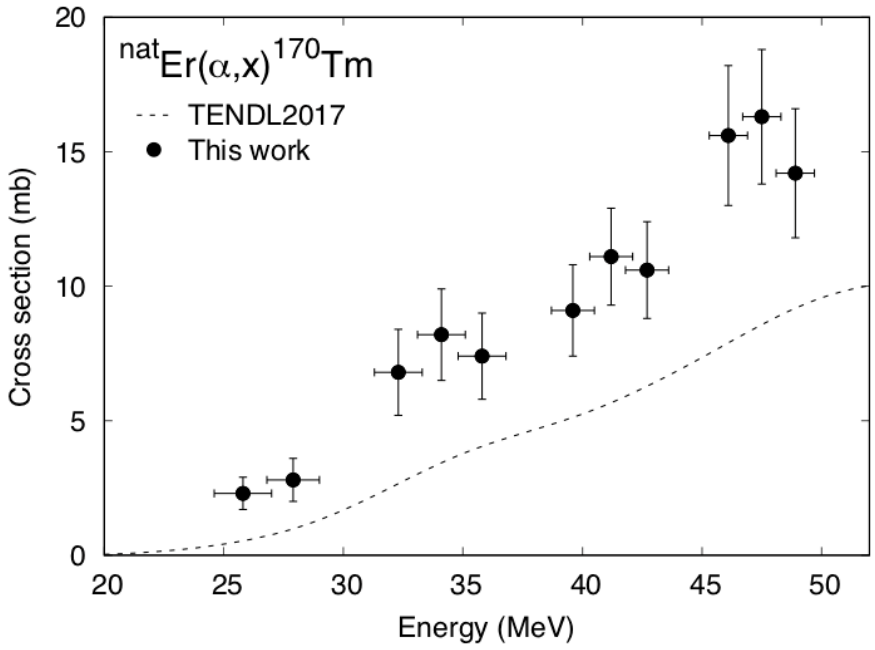

Fig. 5. Excitation function of the ^{nat}Er(α,x)^{170}Tm reaction

3.5 The $^{nat}Er(\alpha,x)^{168}Tm$ reaction

The production cross sections of ^{168}Tm ($T_{1/2}$ = 93.1 d) were derived from the gamma line at 815.99 keV (I_γ = 50.95%). We used the gamma spectra recorded after a cooling time of 247 days. The cross sections are compared with the previous studies (Homma et al., 1980; Sonzogni et al., 1992) and the TENDL-2017 data (Koning et al., 2019). The data of Homma et al. (1980) are very different from the other experimental and calculational data. The data of Sonzogni et al. (1992) are in good agreement with ours. The TENDL-2017 data underestimate the experimental data.

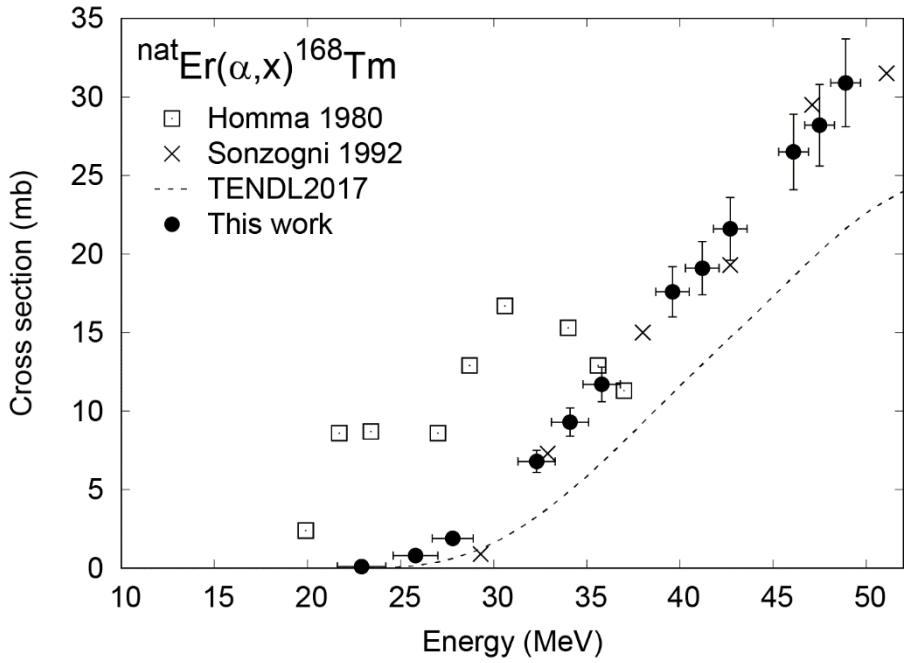

Fig. 6. Excitation function of the $^{nat}Er(\alpha,x)^{168}Tm$ reaction

3.6 The ^{nat}Er(α,x)^{167}Tm reaction

Measurements of the 707.80-keV gamma line (I_γ = 42%) after a cooling time longer than 11 days were used to derive the production cross sections of ^{167}Tm ($T_{1/2}$ = 9.25 d). Its parent ^{167}Yb ($T_{1/2}$ = 17.5 min) decayed completely during the cooling time. The gamma intensity has a large relative uncertainty of 19%, which causes the large uncertainty of our result. The cumulative cross sections are shown in Fig. 7 with the previous experimental data (Homma et al., 1980; Király et al., 2008) and the TENDL-2017 data (Koning et al., 2019). The experimental data of Homma et al. (1980) and Király et al. (2008) slightly deviate to smaller and larger than our data. The TENDL-2017 data are in good agreement with ours below 35 MeV, however lower above 35 MeV.

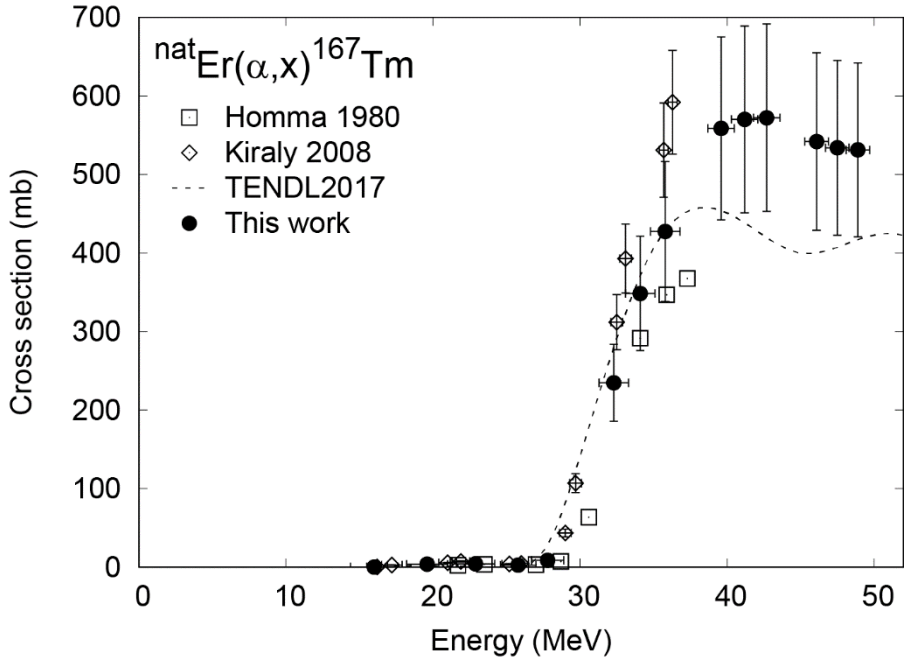

Fig. 7. Excitation function of the ^{nat}Er(α,x)^{167}Tm reaction

3.7 The $^{nat}Er(\alpha,x)^{166}Tm$ reaction

The cross sections for the ^{166}Tm production were derived using measurements of the 778.81-keV gamma line (I_γ = 19.1%) from the decay of its ground state ^{166g}Tm ($T_{1/2}$ = 7.70 h). The metastable state of ^{166}Tm has a short half-life ($T_{1/2}$ = 340 ms) and decayed during the irradiation. The measurements of the gamma line were performed after a cooling time of 11 hours. The contribution of the parent isotope ^{166}Yb ($T_{1/2}$ = 56.7 h) could be estimated from the cross sections determined in section 3.2. The activity of the directly created ^{166}Tm was obtained by subtracting the estimated contribution of ^{166}Yb from the measured activity. The independent cross sections obtained from the corrected activity are shown in Fig. 8. Our results are compared with the TENDL-2017 data (Koning et al., 2019), that by far underestimate our data. No experimental data were found in the EXFOR library.

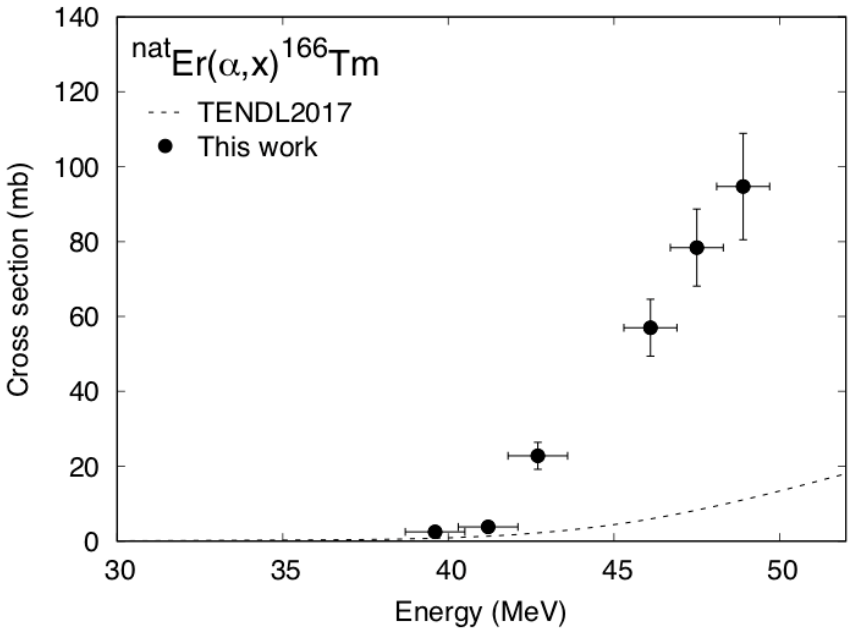

Fig. 8. Excitation function of the $^{nat}Er(\alpha,x)^{166}Tm$ reaction

3.8 The $^{nat}Er(\alpha,x)^{165}Tm$ reaction

The excitation function of the $^{nat}Er(\alpha,x)^{165}Tm$ reaction was derived from measurements of the gamma line at 242.92 keV (I_γ = 35.5%). The spectra measured after a cooling time of 2.2 h were used. During the cooling time, the parent radionuclide ^{165}Yb ($T_{1/2}$ = 9.9 min) decayed to ^{165}Tm ($T_{1/2}$ = 30.06 h). The cumulative cross sections were obtained from the net counts of the gamma line and shown in Fig. 9. The result is compared with the previous studies (Homma et al., 1980; Király et al., 2008) and the TENDL-2017 data (Koning et al., 2019). The data of Király et al. (2008) are nearly consistent with our data. The data of Homma et al. (1980) are smaller than the other experimental data. The TENDL-2017 data show very different behavior above 38 MeV.

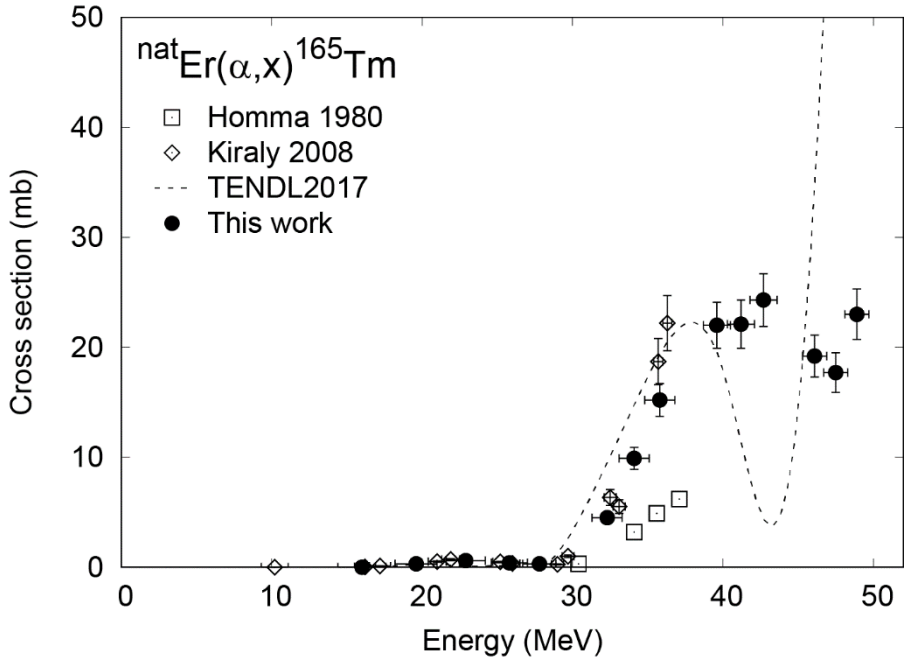

Fig. 9. Excitation function of the $^{nat}Er(\alpha,x)^{165}Tm$ reaction

3.9 Integral yield of ^{169}Yb

The integral yield of ^{169}Yb was deduced from the measured excitation function of the ^{nat}Er(α,x)^{169}Yb reaction and stopping powers calculated by the SRIM code (Ziegler et al., 2008). Physical thick target yield (Otuka and Takács, 2015) up to 48.9 MeV is displayed on Fig. 10 together with the previously published data (Király et al., 2008). Our results are slightly smaller than the previous data, which can be expected from the difference of the cross sections shown in Fig. 2.

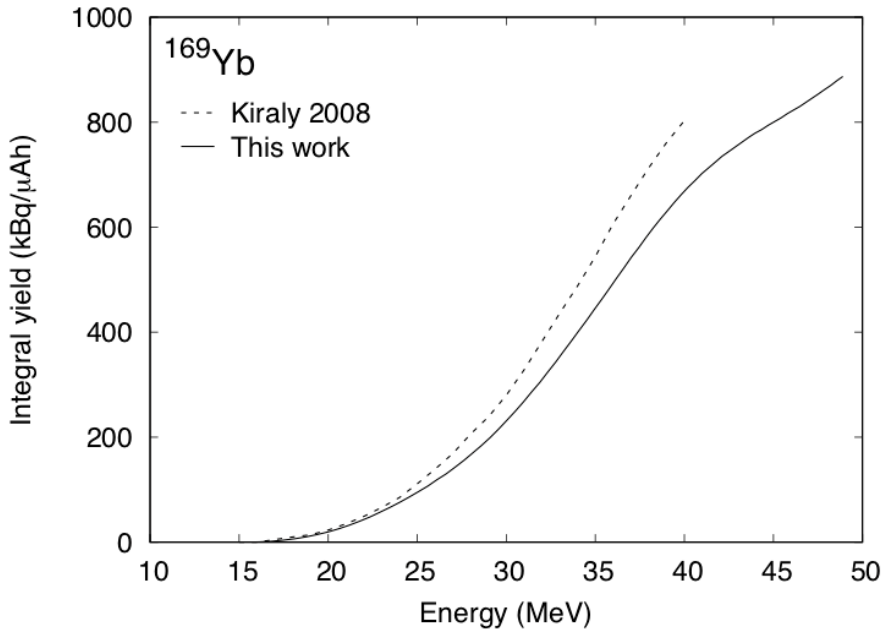

Fig. 10. Integral yield of ^{169}Yb

4. Conclusion

We measured the excitation functions of the alpha-induced reactions on ^{nat}Er up to 48.9 MeV at the RIKEN AVF cyclotron. The production cross sections of ^{169}Yb and co-produced radionuclides, ^{166}Yb and ^{165,166,167,168,170,173}Tm, were determined. These are the first cross section measurements of ^{166,170}Tm. The derived cross sections were compared with the previous studies and the TENDL-2017 data. Based on the measured cross sections, the integral yield of ^{169}Yb was derived. The results obtained in the experiment are expected to contribute to finding the best nuclear reaction to produce the medical radionuclide ^{169}Yb. In addition to the production cross sections, consideration on cost effectiveness is required for practical use as discussed for the neutron capture reaction on enriched ^{168}Yb by Flynn et al. (2019) (Flynn et al., 2019). Based on the current nuclear data, the neutron capture reaction is possibly the best route in case that the costly enriched targets can be prepared and reactivated.

Acknowledgement

This work was carried out at RI Beam Factory operated by RIKEN Nishina Center and CNS, University of Tokyo, Japan. This work was supported by JSPS KAKENHI Grant Number 17K07004.

Declarations of interest

None

Reference

Archenti, A., Wasilevsky, C., De La Vega Vedoya, M., Nassiff, S.J., 1985. (α,xn) Reactions on Natural Erbium. Radiochim. Acta 38, 65–68. https://doi.org/10.1524/ract.1985.38.2.65

Chu, S.Y.F., Ekström, L.P., Firestone, R.B., 1999. The Lund/LBNL Nuclear Data Search [WWW Document]. URL http://nucleardata.nuclear.lu.se/toi/

Flynn, R.T., Adams, Q.E., Hopfensperger, K.M., Wu, X., Xu, W., Kim, Y., 2019. Efficient 169 Yb high-dose-rate brachytherapy source production using reactivation. Med. Phys. 46, 2935–2943. https://doi.org/10.1002/mp.13563

Hermanne, A., Ignatyuk, A. V., Capote, R., Carlson, B. V., Engle, J.W., Kellett, M.A., Kibédi, T., Kim, G., Kondev, F.G., Hussain, M., Lebeda, O., Luca, A., Nagai, Y., Naik, H., Nichols, A.L., Nortier, F.M., Suryanarayana, S. V., Takács, S., Tárkányi, F.T., Verpelli, M., 2018. Reference Cross Sections for Charged-particle Monitor Reactions. Nucl. Data Sheets 148, 338–382. https://doi.org/10.1016/j.nds.2018.02.009

Homma, Y., Sugitani, Y., Matsui, Y., Matsuura, K., Kurata, K., 1980. Cyclotron production of ^{167}Tm from natural erbium and natural holmium. Appl. Radiat. Isot. 31, 505–508. https://doi.org/10.1016/0020-708X(80)90314-2

International Atomic Energy Agency, 2009. LiveChart of Nuclides [WWW Document]. URL https://www-nds.iaea.org/livechart/

Király, B., Tárkányi, F., Takács, S., Hermanne, A., Kovalev, S.F., Ignatyuk, A. V., 2008. Excitation functions of alpha-induced nuclear reactions on natural erbium. Nucl. Instruments Methods Phys. Res. Sect. B 266, 549–554. https://doi.org/10.1016/j.nimb.2007.12.067

Koning, A.J., Rochman, D., Sublet, J., Dzysiuk, N., Fleming, M., Marck, S. van der, 2019. TENDL: Complete Nuclear Data Library for Innovative Nuclear Science and Technology. Nucl. Data Sheets 155, 1–55. https://doi.org/10.1016/j.nds.2019.01.002

Leonard, K.L., DiPetrillo, T.A., Munro, J.J., Wazer, D.E., 2011. A novel ytterbium-169 brachytherapy source and delivery system for use in conjunction with minimally invasive wedge resection of early-stage lung cancer. Brachytherapy 10, 163–169. https://doi.org/10.1016/j.brachy.2010.06.006

National Nuclear Data Center, 2017. Nuclear structure and decay data on-line library, Nudat 2.7 [WWW Document]. URL http://www.nndc.bnl.gov/nudat2/

Otuka, N., Dupont, E., Semkova, V., Pritychenko, B., Blokhin, A.I., Aikawa, M., Babykina, S., Bossant, M., Chen, G., Dunaeva, S., Forrest, R.A., Fukahori, T., Furutachi, N., Ganesan, S., Ge, Z., Gritzay, O.O., Herman, M., Hlavač, S., Kato, K., Lalremruata, B., Lee, Y.O., Makinaga, A., Matsumoto, K., Mikhaylyukova, M., Pikulina, G., Pronyaev, V.G., Saxena, A., Schwerer, O., Simakov, S.P., Soppera, N., Suzuki, R., Takács, S., Tao, X., Taova, S., Tárkányi, F., Varlamov, V. V., Wang, J., Yang, S.C., Zerkin, V., Zhuang, Y., 2014. Towards a More complete and accurate experimental nuclear reaction data library (EXFOR): International collaboration between nuclear reaction data centres (NRDC). Nucl. Data Sheets 120, 272–276. https://doi.org/10.1016/j.nds.2014.07.065

Otuka, N., Takács, S., 2015. Definitions of radioisotope thick target yields. Radiochim. Acta 103, 1–6. https://doi.org/10.1515/ract-2013-2234

Pritychenko, B., Sonzogni, A., 2003. Q-value Calculator (QCalc) [WWW Document]. URL http://www.nndc.bnl.gov/qcalc/

Sonzogni, A.A., Romo, A.S.M.A., Ozafran, M.J., Nassiff, S.J., 1992. Alpha-induced reactions on natural erbium. J. Radioanal. Nucl. Chem. Lett. 165, 295–303. https://doi.org/10.1007/BF02169776

Watanabe, T., Fujimaki, M., Fukunishi, N., Imao, H., Kamigaito, O., Kase, M., Komiyama, M., Sakamoto, N., Suda, K., Wakasugi, M., Yamada, K., 2014. Beam energy and longitudinal beam profile measurement system at the RIBF, in: Proceedings of the 5th International Particle Accelerator Conference (IPAC 2014). pp. 3566–3568.

Ziegler, J.F., Biersack, J.P., Ziegler, M.D., 2008. SRIM: the Stopping and Range of Ions in Matter [WWW Document]. URL http://www.srim.org